World Scientific
www.worldscientific.com

Centrality dependences of soft and hard components of p_t distributions of negative pions in ^{4}He+^{12}C collisions at $4.2A$ GeV/c

Khusniddin K. Olimov[*,†,¶], Akhtar Iqbal[*], Sagdulla L. Lutpullaev[†],
Sayyed A. Hadi[‡], Viktor V. Glagolev[§], B. S. Yuldashev[§]
and Mahnaz Q. Haseeb[*]

[*]*Department of Physics,
COMSATS Institute of Information Technology,
44000 Islamabad, Pakistan*

[†]*Physical-Technical Institute of Uzbek Academy of Sciences,
100084 Tashkent, Uzbekistan*

[‡]*Department of Physics,
Karakoram International University,
Gilgit-Baltistan, Pakistan*

[§]*Laboratory of High Energies,
Joint Institute for Nuclear Research,
141980 Dubna, Russia*
[¶]*olimov@comsats.edu.pk*

The dependences of the shapes of transverse momentum distributions of the negative pions, produced in minimum bias ^{4}He+^{12}C collisions at a momentum of 4.2 GeV/c per nucleon, on collision centrality and fitting range of p_t were analyzed systematically. To study the change in slopes (temperatures) of the p_t spectra of π^- with changing collision centrality and fitting p_t range, the p_t spectra, extracted from the experimental data and quark–gluon string model (QGSM) calculations, were fitted by the one- and two-temperature Hagedorn and Boltzmann functions. Fitting of the experimental p_t distributions of π^- in both the whole p_t and $p_t = 0.1$–1.2 GeV/c intervals required the two-temperature functions for adequate description of spectra, in agreement with the previous findings for different sets of colliding nuclei and various energies. On the whole, the absolute values of the extracted temperatures were lower in case of fitting range $p_t = 0.1$–0.7 GeV/c as compared to the fitting interval $p_t = 0.1$–1.2 GeV/c. The one-temperature functions were sufficient for fitting satisfactorily the experimental p_t distributions of the negative pions in range $p_t = 0.1$–0.7 GeV/c. In contrast to the experimental temperatures, the extracted QGSM temperatures were not sensitive to collision centrality and fitting range of p_t. The collision centrality dependences of

[¶]Corresponding author.

the temperatures of soft ($p_t = 0.1$–$0.5\,\mathrm{GeV}/c$) and hard ($p_t = 0.5$–$1.2\,\mathrm{GeV}/c$) components of the experimental p_t distributions of the negative pions in $^4\mathrm{He}+^{12}\mathrm{C}$ collisions at $4.2A\,\mathrm{GeV}/c$ were studied separately. The extracted temperatures of both soft and hard components of p_t distributions of π^- depended on geometry (size) and degree of overlap of colliding nuclei in peripheral, semicentral and central $^4\mathrm{He}+^{12}\mathrm{C}$ collisions. The temperature of soft p_t component of the negative pions was consistently larger in semicentral and central $^4\mathrm{He}+^{12}\mathrm{C}$ collisions than that in peripheral interactions. The temperature of hard p_t component of π^- in $^4\mathrm{He}+^{12}\mathrm{C}$ collisions decreased consistently with an increase in collision centrality. The physical interpretations of the observed centrality dependences of temperature (T) of soft and hard p_t components of the negative pions in $^4\mathrm{He}+^{12}\mathrm{C}$ collisions were given.

1. Introduction

The threshold energies for pion production in nucleon–nucleon (*NN*) collision are 290 and 280\,MeV for charged and neutral pions, respectively.[1] Therefore, pions are the most abundantly produced particles at collisions of intermediate and high energy nuclei. Pion multiplicity measurements at the BEVALAC were used to derive important information on the nuclear equation-of-state (EOS).[2,3] The basic idea was to use the pions as a thermometer and the incident energy as a measure of the pressure. The temperature (T) and density of the nuclear matter are among the main parameters of the nuclear EOS. The slopes of the energy or transverse momentum distributions of these hadrons are usually analyzed to estimate their temperatures. Pion production was also suggested as a probe of compressional energy in the high-density phase of near head-on collisions.[4] Investigation of the properties of pions, produced predominantly in relativistic nuclear collisions, is also important for understanding the dynamics of the nuclear collisions.

The negatively charged pions are produced abundantly at the energies of the Dubna synchrophasotron and can be unambiguously separated from the other products of nuclear collisions. The excitation and decay of baryon resonances were shown to be one of the main processes responsible for pion production in relativistic nuclear collisions.[5–8] In Refs. 5–13, it was shown that the significant fraction of pions produced in experiments on 2\,m propane and 1\,m hydrogen bubble chambers of the Joint Institute for Nuclear Research (JINR, Dubna, Russia) was generated from decay of delta (Δ) resonances. It was demonstrated in Refs. 14–18 that the Δ resonances play an important role in pion production in relativistic heavy ion collisions. The decay kinematics of Δ resonances was shown to be responsible for low transverse momentum enhancement of pion spectra in hadron–nucleus and nucleus–nucleus collisions at incident beam energies from 1\,Gev to 15\,GeV per nucleon.[6,17,18] It was deduced that pions coming from Δ decay populated mainly the low transverse momentum part of the p_t spectra of pions.[6,17,18]

In Ref. 19, the spectral temperatures of π^- mesons produced in d+^{12}C, ^{4}He+^{12}C and ^{12}C+^{12}C collisions at $4.2A\,\mathrm{GeV}/c$ were extracted by fitting noninvariant center-of-mass (cm) energy spectra of π^- mesons with Maxwell–Boltzmann distribution function. Analysis of rapidity and angular dependences of the spectral temperatures of the negative pions produced in ^{12}C+^{12}C collisions at $4.2A\,\mathrm{GeV}/c$ was performed in Ref. 20. The temperatures of the negative pions were extracted and analyzed for collisions of different sets of nuclei at various energies in the past.[19,21−25] Analysis of transverse momentum as well as transverse mass distributions was preferred for estimating the hadron temperatures due to their Lorentz invariance with respect to longitudinal boosts.[21,24,26,27]

The transverse momentum as well as cm energy spectra of pions, produced in relativistic hadron–nucleus and nucleus–nucleus collisions, demonstrated the two-temperature shape.[19−21,23,24,27−29] The lower temperature (T_1) component was dominant contributing $\sim$(80–90)% to the total pion spectra, and the higher temperature (T_2) one accounted for the remaining $\sim$(10–20)% part.[19,21,27−29] However, practically no centrality dependence of these temperatures could be revealed from fitting the whole or main part of p_t and cm energy distributions of pions in the past.[19,27−29] The reason for this could be interplay of the temperatures of soft and hard components of pion distributions while performing combined two-temperature model fits. It is, therefore, of particular interest to study the centrality dependence of the slopes (temperatures) of p_t distributions of pions, produced in relativistic nuclear collisions, separately in soft and hard p_t regions.

The present paper continues our recent works[20,27−30] devoted to investigation of various characteristics of transverse momentum and rapidity distributions of π^- mesons produced in nucleus–nucleus collisions at $4.2\,\mathrm{GeV}/c$ per nucleon. We aim to investigate systematically the dependences of the shapes of the experimental p_t distributions of the negative pions, produced in ^{4}He+^{12}C collisions at $4.2A\,\mathrm{GeV}/c$ per nucleon, on collision centrality and fitting range of p_t. The main goal of the present analysis is to reveal and interpret the collision centrality dependences of T of soft and hard components of p_t distributions of π^- produced in ^{4}He+^{12}C collisions at $4.2A\,\mathrm{GeV}/c$ ($\sqrt{s_{nn}} = 3.14\,\mathrm{GeV}$, $E_{\mathrm{kin}} \approx 3.4A\,\mathrm{GeV}$). To analyze quantitatively the changes in slopes (temperatures) of the p_t spectra of π^- mesons with changing centrality of ^{4}He+^{12}C collisions and fitting range of p_t, the extracted p_t distributions will be fitted by one- and two-temperature Hagedorn and Boltzmann functions, which were demonstrated to describe adequately the pion p_t distributions in Refs. 20, 24, 27–29. It is necessary to mention that the systematic analysis of the p_t distributions of π^- mesons produced in ^{12}C+^{12}C and ^{12}C+^{181}Ta collisions at $4.2A\,\mathrm{GeV}/c$ at different collision centralities and various pion rapidity ranges was made in recent works.[28,29]

2. Experimental Procedures and Analysis

The data analyzed in the present paper were obtained using $2\,\mathrm{m}$ propane (C_3H_8) bubble chamber of Laboratory of High Energies of JINR (Dubna, Russia). The $2\,\mathrm{m}$

propane bubble chamber was placed in a magnetic field of strength 1.5 T.[28,31−38] The bubble chamber was irradiated with beams of ^{4}He nuclei accelerated to a momentum of 4.2 GeV/c per nucleon at Dubna synchrophasotron. Methods of selection of inelastic ^{4}He+^{12}C collision events in this experiment were given in detail in Refs. 31–38. Threshold for detection of π^- mesons produced in ^{4}He+^{12}C collisions was ≈ 70 MeV/c. In some momentum and angular intervals, the particles could not be detected with 100% efficiency. To account for small losses of particles emitted under large angles to object plane of the camera, the relevant corrections were introduced.[31−38] The average uncertainty in measurement of emission angle of the negative pions was 0.8°. The mean relative uncertainty of momentum measurement of π^- mesons from the curvature of their tracks in propane bubble chamber was $\approx 6\%$. All the negative particles, except those identified as electrons, were considered to be π^- mesons. Admixtures of unidentified electrons and negative strange particles among them did not exceed 5%. In our experiment, the spectator protons are protons with momenta $p > 3$ GeV/c and emission angle $\theta < 4°$ (projectile spectators), and protons with momenta $p < 0.3$ GeV/c (target spectators) in the laboratory frame.[31−38] Hence, the participant protons are the protons which remain after elimination of the spectator protons. Statistics of the experimental data analyzed in the present work consist of 11,974 ^{4}He+^{12}C minimum bias inelastic collision events with practically all the secondary charged particles detected and measured under 4π acceptance.

Table 1 presents a comparison of the mean multiplicities per event of the negative pions and participant protons and the average values of rapidity and transverse momentum of π^- mesons in minimum bias ^{4}He+^{12}C collisions at 4.2A GeV/c both in the experiment and quark–gluon string model (QGSM).[39−42]

The QGSM was developed to describe hadron–nucleus and nucleus–nucleus collisions at high energies.[39−42] In the QGSM, hadron production occurs via formation and decay of quark–gluon strings. This model is used as a basic process for generation of hadron–hadron collisions. In this model, nucleus–nucleus collisions are considered as a set of independent interactions of nucleons from projectile and target nuclei and of stable secondary hadrons and resonances. In the present work, the version of QGSM[40] adapted to the range of intermediate energies ($\sqrt{S_{nn}} \le 4$ GeV) was used. The incident momentum of 4.2 GeV/c per nucleon for nucleus–nucleus collisions analyzed in the present work corresponds to incident kinetic energy 3.37 GeV

Table 1. Mean multiplicities per event of the negative pions and participant protons and the average values of rapidity and transverse momentum of π^- mesons in ^{4}He+^{12}C collisions at 4.2 GeV/c per nucleon. The mean rapidities are calculated in cm of nucleon–nucleon collisions at 4.2 GeV/c. Only statistical errors are given here and at tables that follow.

Type	$\langle n(\pi^-)\rangle$	$\langle n_{\text{part.prot.}}\rangle$	$\langle y_{\text{cm}}(\pi^-)\rangle$	$\langle p_t(\pi^-)\rangle$, GeV/$c$
Experiment	1.02 ± 0.01	2.83 ± 0.02	-0.090 ± 0.007	0.247 ± 0.002
QGSM	0.99 ± 0.01	2.60 ± 0.01	-0.082 ± 0.007	0.224 ± 0.001

per nucleon and nucleon–nucleon cm energy $\sqrt{S_{nn}} = 3.14$ GeV. The QGSM is based on Regge and string phenomenologies of particle production in inelastic binary hadron collisions. To describe the evolution of the hadron and quark–gluon phases, a coupled system of Boltzmann-like kinetic equations was used in the model. The nuclear collisions were treated as a superposition of independent interactions of the projectile and target nucleons, stable hadrons and short-lived resonances. Resonant reactions like $\pi + N \to \Delta$, pion absorption by NN quasi-deuteron pairs and also $\pi + \pi \to \rho$ reactions were taken into account in the model. The time of formation of hadrons was also included in QGSM. The masses of strings at intermediate energies are very small. At $\sqrt{S_{nn}} = 3.14$ GeV the masses of strings are smaller than 2 GeV, and these strings fragment predominantly ($\sim$90%) through two particle decay channel. In the QGSM, Δ^0 and Δ^- resonances and ρ^-, ρ^0, ω, η and η' as well as the so-called "prompt" π^- mesons are sources of the negative pions. "Prompt" π^- mesons are produced directly in hadron–hadron collisions. These can be primary or secondary NN collisions ($NN \to NN\pi$), or interactions of secondary mesons with nucleons ($\rho N \to \pi N$). The decay of excited recoil nuclear fragments and a coupling of nucleons inside the nucleus were not taken into account in QGSM. More detailed description of QGSM can be found in Refs. 39–42. We used 15,000 inelastic minimum bias ^{4}He$+^{12}$C collision events at $4.2A$ GeV$/c$, simulated using QGSM, for comparison with the corresponding experimental data.

The transverse momentum and rapidity distributions of the negative pions in minimum bias ^{4}He$+^{12}$C collisions at a momentum of $4.2A$ GeV$/c$ are presented in Fig. 1. As can be seen from Fig. 1(a), the experimental transverse momentum distribution of π^- mesons is described satisfactorily by the QGSM calculations in

(a) (b)
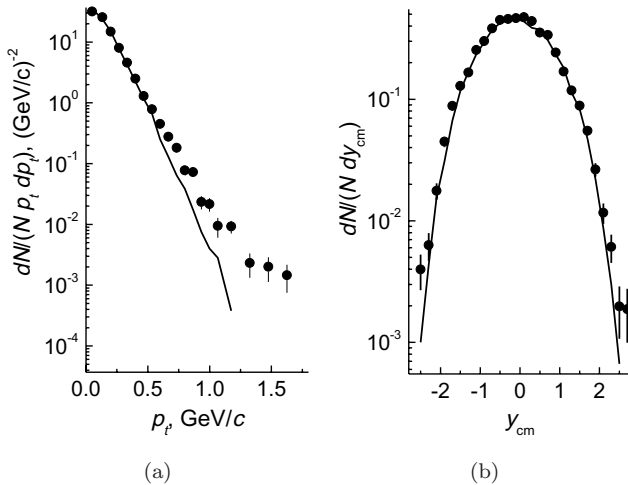
Fig. 1.   The experimental (a) transverse momentum and (b) rapidity distributions of the negative pions produced in minimum bias ^{4}He$+^{12}$C collisions ($\bullet$) at 4.2 GeV$/c$ per nucleon. The corresponding calculated QGSM spectra are given by the solid lines. All the spectra are normalized per one inelastic collision event.

region $p_t < 0.8\,\text{GeV}/c$. The rapidity distribution in Fig. 1(b) is given in cm of nucleon–nucleon collisions at $4.2\,\text{GeV}/c$ (the rapidity of the cm of nucleon–nucleon collision is $y_{\text{cm}} \approx 1.1$ at this incident momentum). Figure 1(a) also shows that the QGSM underestimates the experimental p_t spectrum of π^- mesons in region $p_t > 0.8\,\text{GeV}/c$. It is important to mention that another model — modified FRITIOF model,[39,42−45] specifically modified for description of the nucleus–nucleus collisions at incident energies of the order of a few GeV per nucleon, also underestimates this high p_t part of the pion distribution.[27,46] It was shown earlier[27] that the fitting of the p_t spectrum of π^- in $d+^{12}$C, ^{4}He$+^{12}$C and ^{12}C$+^{12}$C collisions at $4.2A\,\text{GeV}/c$ with the two-temperature Hagedorn function resulted in the lower values of T_1 and T_2 for both QGSM and modified FRITIOF model spectra as compared to the experiment. As seen from Fig. 1(b), QGSM describes quite satisfactorily the experimental rapidity distribution of π^- in ^{4}He$+^{12}$C collisions. Comparison of the average values of rapidity and transverse momentum of the negative pions, given in Table 1, supports the above observations.

We fitted the transverse momentum spectra of π^- mesons produced in ^{4}He$+^{12}$C collisions at a momentum of $4.2\,\text{GeV}/c$ per nucleon by Hagedorn and Boltzmann functions, shown[20,24,27−29] to describe successfully the p_t distributions of pions. The Hagedorn thermodynamic model[26,47] allows for a set of fireballs displaced from each other in rapidity. In this model, particles with different momenta freeze out within a volume that is of universal magnitude when assessed in the rest frame for any given momentum, being the distribution in transverse momentum of the shape $dN/dp_t = \text{const} \cdot p_t \cdot m_t \cdot K_1(m_t/T) \approx \text{const} \cdot p_t \cdot (m_t \cdot T)^{1/2} \cdot \exp(-m_t/T)$, where K_1 is the Macdonald function, $m_t = \sqrt{m^2 + p_t^2}$ is the transverse mass, T is the spectral temperature. The above approximation is valid for $m_t \gg T$. Thus, the Hagedorn thermodynamic model[26,47] predicts that the normalized transverse momentum (p_t) distribution of hadrons can be described using the expression (assuming $m_t \gg T$):

$$\frac{dN}{N p_t dp_t} = A \cdot (m_t T)^{1/2} \exp\left(-\frac{m_t}{T}\right), \tag{1}$$

where N (depending on the choice of normalization) is either the total number of inelastic events or the total number of the respective hadrons and A is the fitting constant. This relation (1) will be referred to as the one-temperature Hagedorn function throughout the present paper. Correspondingly, in case of two-temperatures, T_1 and T_2, the above formula is modified as

$$\frac{dN}{N p_t dp_t} = A_1 \cdot (m_t T_1)^{1/2} \exp\left(-\frac{m_t}{T_1}\right) + A_2 \cdot (m_t T_2)^{1/2} \exp\left(-\frac{m_t}{T_2}\right), \tag{2}$$

referred to as the two-temperature Hagedorn function in this work.

The Boltzmann model assumes that the transverse momentum distributions of hadrons can be fitted using m_t Boltzmann distribution function given by

$$\frac{dN}{N p_t dp_t} = A m_t \exp\left(-\frac{m_t}{T}\right), \tag{3}$$

referred as the one-temperature Boltzmann function in the present paper. In case of two-temperatures, T_1 and T_2, the above formula is modified as

$$\frac{dN}{Np_t dp_t} = A_1 \cdot m_t \exp\left(-\frac{m_t}{T_1}\right) + A_2 \cdot m_t \exp\left(-\frac{m_t}{T_2}\right). \tag{4}$$

The experimental p_t distribution of the negative pions produced in minimum bias ^{4}He$+^{12}$C collisions at $4.2A$ GeV$/c$ and the corresponding fits in the whole p_t range by the one-temperature and two-temperature Hagedorn and Boltzmann functions are presented in Fig. 2. As can be seen from Fig. 2, the two-temperature Hagedorn and Boltzmann functions fit the total p_t distribution of the negative pions markedly better as compared to the corresponding one-temperature functions.
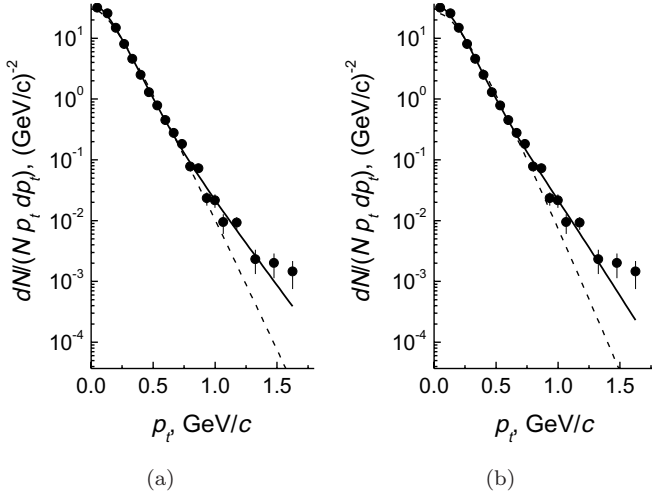

(a)   (b)

Fig. 2. The experimental transverse momentum distribution ($\bullet$) of the negative pions produced in minimum bias ^{4}He$+^{12}$C collisions at 4.2 GeV$/c$ per nucleon and the corresponding fits in the whole p_t range by the one-temperature (dashed lines) and two-temperature (solid lines) (a) Hagedorn and (b) Boltzmann functions. The distribution is normalized per one inelastic collision event.

Table 2. The parameters extracted from fitting the transverse momentum distribution of the negative pions in the whole p_t range in minimum bias ^{4}He$+^{12}$C collisions at $4.2A$ GeV$/c$ by the one- and two-temperature Hagedorn and Boltzmann functions.

Fitting function	Type	A_1 (GeV)$^{-1}$	T_1 (MeV)	A_2 (GeV)$^{-1}$	T_2 (MeV)	$\chi^2/n.d.f.$	R^2
1T Hagedorn	Exper.	1102 ± 65	$\mathbf{97 \pm 1}$	—	—	4.19	0.96
	QGSM	1843 ± 45	$\mathbf{84 \pm 1}$	—	—	1.35	0.99
2T Hagedorn	Exper.	1713 ± 186	$\mathbf{83 \pm 4}$	43 ± 33	$\mathbf{150 \pm 15}$	1.43	0.99
	QGSM	1314 ± 2102	$\mathbf{87 \pm 10}$	702 ± 1819	$\mathbf{70 \pm 46}$	1.43	0.99
1T Boltzmann	Exper.	974 ± 56	$\mathbf{86 \pm 1}$	—	—	6.34	0.95
	QGSM	1652 ± 38	$\mathbf{74 \pm 1}$	—	—	4.05	0.99
2T Boltzmann	Exper.	1811 ± 204	$\mathbf{68 \pm 3}$	71 ± 33	$\mathbf{124 \pm 8}$	1.44	0.99
	QGSM	1706 ± 223	$\mathbf{53 \pm 7}$	822 ± 267	$\mathbf{82 \pm 3}$	1.35	0.99

Parameters extracted from fitting the total p_t distribution of the negative pions in the whole p_t range in minimum bias ^{4}He+^{12}C collisions at $4.2A\,\text{GeV}/c$ by the two-temperature and one-temperature Hagedorn and Boltzmann functions are presented in Table 2. R^2 factor in Table 2 is given by relation $R^2 = 1 - \frac{SS_E}{SS_T}$, where $SS_E = \sum_{i=1}^{n} \left(y_i^{\text{exp}} - y_i^{\text{fit}}\right)^2$ is the sum of squared errors, $SS_T = \sum_{i=1}^{n} \left(y_i^{\text{exp}} - \bar{y}\right)^2$ is the total sum of squares, y_i^{exp} and y_i^{fit} are the original (experimental) and fit (model) data, respectively, and $\bar{y} = \frac{1}{n} \sum_{i=1}^{n} y_i^{\text{exp}}$ is the mean value of the experimental data. As the deviation between the experimental and fit data becomes smaller, R^2 factor approaches to one. Hence, the closer R^2 factor value to one, the better is the fit quality. Comparison of $\chi^2/n.d.f.$ and R^2 factor values, given in Table 2, confirms that the two-temperature Hagedorn and two-temperature Boltzmann function fits describe the experimental p_t distribution much better compared to the corresponding one-temperature function fits. This is in agreement with the earlier works,[19–21,23,24,27–29] where the transverse momentum as well as cm energy spectra of pions, produced in relativistic nuclear collisions, demonstrated the two-temperature shapes. Reference 21 revealed the two-temperature shape of cm kinetic energy spectra of the negative pions in Ar+KCl collisions at $1.8\,\text{GeV}/\text{nucleon}$. The occurrence of two temperatures, T_1 and T_2, in this work was interpreted as due to two channels of pion production: Pions coming from Δ resonance decay (T_1) and directly produced pions (T_2). In Ref. 23, the two-temperature shape of kinetic energy spectrum of pions emitted at $90°$ in cm of central La+La collisions at $1.35\,\text{GeV}/\text{nucleon}$ was explained as due to different contributions of deltas originated from the early and later stages of heavy ion reactions. The two-temperature behavior was also observed for cm energy as well as p_t spectra of π^- mesons produced in central Mg+Mg collisions[24] at incident momenta of 4.2–$4.3A\,\text{GeV}/c$.

It would be oversimplified to believe that the origin of pions in a minimum bias sample of ^{4}He+^{12}C collisions could only be described by two thermal sources. The phenomenon of collective flow has become the well-established and an important feature of relativistic heavy ion collisions. Inverse slope parameter, T, or an apparent temperature of the emitting source, of transverse mass spectra of hadrons was shown to consist of two components: A thermal part, T_{thermal} and a second part resembling the collective expansion with an average transverse velocity $\langle \beta_t \rangle$.[48] The collective flow of protons and negative pions was observed experimentally also in He+C, C+C, C+Ne, C+Cu and C+Ta collisions within the momentum range of $4.2A$–$4.5A\,\text{GeV}/c$.[35,49,50] Hence, the observed shapes of the transverse momentum distribution of the negative pions produced in ^{4}He+^{12}C collisions at $4.2A\,\text{GeV}/c$ could also be influenced by the collective flow effects. The two-temperature shape of pion spectrum could also be explained qualitatively as due to two pion types: Pions, emitted from the "hot" core of collision zone at initial collision stage, and other pions, coming later from expansion and freeze-out of a highly compressed nuclear matter, or a fireball, created in central or semicentral nucleus–nucleus collisions. The low temperature part of pion spectrum can also be thought as due to contribution

of mixture of pions, originated from expansion and freeze-out of a fireball, with "cold" pions coming from decay of resonances at a later stage of collision. And, the high temperature part of pion spectrum can likely be due to pions produced in semi(hard) nucleon–nucleon collisions.

The spectral temperatures (T_1, T_2) of π^- mesons in minimum bias ^{4}He$+^{12}$C collisions at $4.2A\,$GeV$/c$ and their relative contributions (R_1, R_2) extracted in the present work from fitting the p_t distribution by the two-temperature Hagedorn and two-temperature Boltzmann functions are shown in Table 3. The corresponding results obtained in Ref. 19 from fitting the noninvariant cm energy distribution of the negative pions in minimum bias ^{4}He$+^{12}$C collisions at the same initial momentum using two-temperature Maxwell–Boltzmann distribution function are also shown for a comparison in this table. The relative contributions, R, of the different temperatures to the total negative pion multiplicity were calculated over the total transverse momentum interval ($R_i = c_i/(c_1 + c_2)$), where $c_i = A_i \cdot \int (m_t T_i)^{1/2} \exp(-\frac{m_t}{T_i}) dp_t$ and $c_i = A_i \cdot \int m_t \exp(-\frac{m_t}{T_i}) dp_t (i = 1, 2)$ are for the case of Hagedorn and Boltzmann function fits, respectively). It is necessary to mention that the statistics of ^{4}He$+^{12}$C collisions used in Ref. 19 was 4849 inelastic collision events, which is more than two times lesser than the statistics used in the present analysis. As seen from Table 3, the values of the spectral temperatures (T_1, T_2) extracted in the present work from fitting the p_t distribution by the two-temperature Hagedorn and the two-temperature Boltzmann functions proved to be noticeably lower compared to the corresponding values obtained in Ref. 19 from fitting the noninvariant cm energy spectrum of π^- by Maxwell–Boltzmann distribution function. Especially the value of T_2 obtained in Ref. 19 is quite large for such relatively small collision system and energy. This is likely due to the influence of longitudinal motion on the energy spectra of π^- mesons, whereas p_t distributions are Lorentz invariant with respect to longitudinal boosts. As seen from Table 3, the dominant contribution ($R_1 \sim 90\%$) to the total π^- multiplicity in ^{4}He$+^{12}$C collisions is given by $T_1 \sim (68 - 83) \pm 5\,$MeV. The values of R_1 obtained in the present work agreed well with the corresponding value extracted in Ref. 19. As seen from Table 3, the fits by Boltzmann function result in slightly lower values of T compared to those by Hagedorn function. This tendency was also observed in our recent works when comparing the fits by Hagedorn and Boltzmann functions of the

Table 3. The spectral temperatures (T) of the negative pions in minimum bias ^{4}He$+^{12}$C collisions at $4.2A\,$GeV$/c$ and their relative contributions (R) extracted in the present work from fitting their experimental transverse momentum distribution in the whole p_t range by the two-temperature Hagedorn and Boltzmann functions compared to the corresponding values obtained in Ref. 19 from fitting the noninvariant cm energy spectra of the negative pions by Maxwell–Boltzmann distribution function.

Fitting function	T_1 (MeV)	R_1(%)	T_2 (MeV)	R_2 (%)	χ^2/n.d.f.	R^2
Hagedorn	$\mathbf{83 \pm 4}$	89 ± 14	$\mathbf{150 \pm 15}$	11 ± 8	1.43	0.99
Boltzmann	$\mathbf{68 \pm 3}$	85 ± 13	$\mathbf{124 \pm 8}$	15 ± 7	1.44	0.99
Maxwell–Boltzmann	$\mathbf{94 \pm 6}$	85 ± 11	$\mathbf{173 \pm 22}$	15 ± 11	0.54	—

p_t distributions of the negative pions in ^{12}C+^{12}C (Ref. 28) and ^{12}C+^{181}Ta (Ref. 29) collisions at $4.2A$ GeV/c.

It is seen from Fig. 2 that the p_t distribution of the negative pions with $p_t \leq 1.2$ GeV/c is characterized by good enough statistics of π^- mesons and, hence, by sufficiently low statistical errors. Due to the lower momentum threshold of detection of pions $p_{\text{thresh}} \approx 70$ MeV/c, it was natural to fit the transverse momentum distributions of pions in range $p_t = 0.1$–1.2 GeV/c, where pions are detected and measured with practically 100% efficiency.[28,29] We fitted the p_t distribution of π^- in this p_t range in minimum bias ^{4}He+^{12}C collisions at $4.2A$ GeV/c both in experiment and QGSM by the one- and two-temperature Hagedorn and Boltzmann functions given in expressions (1)–(4). Parameters extracted from fitting the total p_t distribution of the negative pions in range $p_t = 0.1$–1.2 GeV/c in minimum bias ^{4}He+^{12}C collisions at $4.2A$ GeV/c by these functions are given in Table 4. As seen from comparison of Tables 2 and 4, the values of T_1 and T_2 obtained from fitting the p_t distribution of the negative pions in range $p_t = 0.1$–1.2 GeV/c by the two-temperature Hagedorn and Boltzmann functions are generally lower than the corresponding temperatures extracted from fitting in the whole p_t range. At the same time, as seen from Table 4, the QGSM underestimates noticeably the values of T_1 and T_2 obtained from fitting the p_t distribution of the negative pions in experiment.

We analyzed quantitatively the change in shapes (slopes) of the p_t distributions of π^- with an increase in collision centrality, which corresponds to decrease of the impact parameter of collision. Since impact parameter cannot be measured directly, we used the number of participant protons N_p to characterize the collision centrality. We followed Refs. 27–29, 31, 51 to define the peripheral collision events to be those in which $N_p \leq \langle n_{\text{part.prot.}} \rangle$, and the central collisions as the collision events with $N_p \geq 2\langle n_{\text{part.prot.}} \rangle$, where $\langle n_{\text{part.prot.}} \rangle$ is the mean multiplicity per event of participant protons, and the semicentral collisions come in between these two multiplicity intervals. Reference 51 showed that the central ^{12}C+^{181}Ta collisions at $4.2A$ GeV/c selected using the above criterion were characterized by complete

Table 4. The parameters extracted from fitting the p_t distributions of the negative pions in minimum bias ^{4}He+^{12}C collisions at $4.2A$ GeV/c by the one- and two-temperature Hagedorn and Boltzmann functions in range $p_t = 0.1$–1.2 GeV/c.

Fitting function	Type	A_1 (GeV)$^{-1}$	T_1 (MeV)	A_2 (GeV)$^{-1}$	T_2 (MeV)	$\chi^2/n.d.f.$	R^2
1T Hagedorn	Exper.	1027 ± 72	$\mathbf{98 \pm 1}$	—	—	4.27	0.97
	QGSM	1838 ± 56	$\mathbf{84 \pm 1}$	—	—	1.45	0.99
2T Hagedorn	Exper.	2897 ± 915	$\mathbf{67 \pm 8}$	225 ± 116	$\mathbf{122 \pm 8}$	1.15	0.99
	QGSM	1123 ± 2041	$\mathbf{51 \pm 38}$	1577 ± 435	$\mathbf{86 \pm 3}$	1.46	0.99
1T Boltzmann	Exper.	842 ± 57	$\mathbf{88 \pm 1}$	—	—	6.26	0.95
	QGSM	1539 ± 44	$\mathbf{75 \pm 1}$	—	—	3.22	0.99
2T Boltzmann	Exper.	2661 ± 678	$\mathbf{59 \pm 5}$	160 ± 62	$\mathbf{112 \pm 6}$	1.17	0.99
	QGSM	2071 ± 869	$\mathbf{49 \pm 10}$	916 ± 255	$\mathbf{81 \pm 3}$	1.42	0.99

projectile stopping, because in these collisions the average number of interacting projectile nucleons (the average number of participant nucleons from projectile nucleus) was very close to the total number of nucleons in projectile carbon. Fractions of central, semicentral and peripheral ^{4}He$+^{12}$C collision events, relative to the total inelastic cross-section, obtained for both experimental and QGSM data are presented in Table 5. As seen from Table 5, the experimental and corresponding QGSM fractions of peripheral, semicentral and central ^{4}He$+^{12}$C collision events agree with each other.

The parameters extracted from fitting the p_t distributions of the negative pions in range $p_t = 0.1$–1.2 GeV/c in peripheral, semicentral and central ^{4}He$+^{12}$C collisions at $4.2A$ GeV/c by two-temperature functions are presented in Table 6. As seen from Table 6, the fits of the p_t distributions by the two-temperature Hagedorn and Boltzmann functions are compatible with each other, within fitting uncertainties, in peripheral, semicentral and central ^{4}He$+^{12}$C collisions. As observed from Table 6, the absolute values of T_1 and T_2 extracted in peripheral collisions proved to be larger compared to those in semicentral and central collisions. This observation could be understood if we recall that the temperature is the measure of the mean kinetic energy of particles, and that we have asymmetric collision system with the target carbon nucleus heavier than light projectile helium-4 nucleus ($A_p < A_t$). In case of central ^{4}He$+^{12}$C collisions, the collision energy is distributed, on the average, among noticeably larger number of interacting target nucleons and produced pions compared to peripheral ^{4}He$+^{12}$C collisions, which results in lower mean kinetic energies of π^- in central ^{4}He$+^{12}$C collisions as compared to the peripheral interactions. The experimental p_t distributions of the negative pions produced in peripheral, semicentral and central ^{4}He$+^{12}$C collisions and the corresponding fits

Table 5. Fractions of central, semicentral and peripheral ^{4}He$+^{12}$C collisions at $4.2A$ GeV/c, relative to the total inelastic cross-section.

Peripheral collisions (%)		Semicentral collisions (%)		Central collisions (%)	
Experiment	QGSM	Experiment	QGSM	Experiment	QGSM
54 ± 1	54 ± 1	37 ± 1	38 ± 1	9 ± 1	8 ± 1

Table 6. The parameters extracted from fitting the experimental p_t distributions of the negative pions in peripheral, semicentral and central ^{4}He$+^{12}$C collisions at $4.2A$ GeV/c by the two-temperature Hagedorn and Boltzmann functions in range $p_t = 0.1$–1.2 GeV/c.

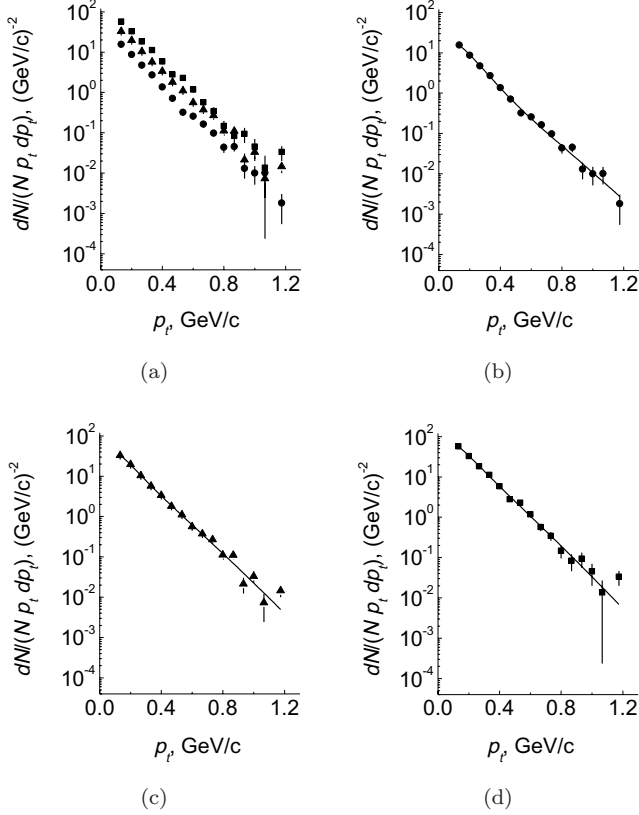| Fitting function	Collision type	A_1 (GeV)$^{-1}$	T_1 (MeV)	A_2 (GeV)$^{-1}$	T_2 (MeV)	$\chi^2/n.d.f.$	R^2
Hagedorn	Peripheral	1921 ± 625	$\mathbf{67 \pm 8}$	97 ± 74	$\mathbf{125 \pm 12}$	0.99	0.99
	Semicentral	5144 ± 3195	$\mathbf{57 \pm 11}$	554 ± 228	$\mathbf{112 \pm 6}$	1.53	0.99
	Central	6915 ± 6351	$\mathbf{59 \pm 20}$	1164 ± 824	$\mathbf{109 \pm 10}$	0.97	0.99
Boltzmann	Peripheral	1680 ± 442	$\mathbf{60 \pm 5}$	68 ± 40	$\mathbf{115 \pm 9}$	0.95	0.99
	Semicentral	4410 ± 1858	$\mathbf{53 \pm 7}$	358 ± 129	$\mathbf{104 \pm 5}$	1.52	0.99
	Central	6593 ± 4078	$\mathbf{54 \pm 11}$	768 ± 446	$\mathbf{100 \pm 8}$	0.98	0.99

Fig. 3. The experimental transverse momentum distributions of the negative pions produced in peripheral (●) ((a) and (b)), semicentral (▲) ((a) and (c)) and central (■) ((a) and (d)) ^{4}He+^{12}C collisions at $4.2\,\mathrm{GeV}/c$ per nucleon and the corresponding fits in range $p_t = 0.1$–$1.2\,\mathrm{GeV}/c$ by the two-temperature Boltzmann function (solid lines). All the spectra are normalized per one inelastic collision event.

in range $p_t = 0.1$–$1.2\,\mathrm{GeV}/c$ by the two-temperature Boltzmann function are given in Fig. 3. As observed from Fig. 3, the two-temperature Boltzmann function fits very well the p_t distributions of π^- in peripheral, semicentral and central ^{4}He+^{12}C collisions.

Table 7 presents the collision centrality dependence of the parameters extracted from fitting the p_t distributions of the negative pions in peripheral, semicentral and central ^{4}He+^{12}C collisions by the one-temperature Hagedorn and Boltzmann functions in range $p_t = 0.1$–$1.2\,\mathrm{GeV}/c$. It is seen from Table 7 that the absolute values of T proved to be consistently and noticeably larger in case of semicentral and central collisions as compared to peripheral interactions. It is necessary to mention that the temperatures extracted from QGSM spectra, as seen from Table 7, did not show any dependence on collision centrality.

To examine the influence of the fitting range of p_t on the extracted values of T of π^- for three ^{4}He+^{12}C collision centrality groups, the p_t distributions

Table 7. The parameters extracted from fitting the p_t distributions of the negative pions in peripheral, semicentral and central ^{4}He+^{12}C collisions at $4.2A$ GeV/c by one-temperature Hagedorn and Boltzmann functions in range $p_t = 0.1$–1.2 GeV/c.

Fitting function	Collision type	Type	A (GeV)$^{-1}$	T (MeV)	$\chi^2/n.d.f.$	R^2
Hagedorn	Peripheral	Exper.	829 ± 77	$\mathbf{91 \pm 2}$	2.92	0.96
		QGSM	939 ± 53	$\mathbf{84 \pm 1}$	1.65	0.99
	Semicentral	Exper.	1421 ± 114	$\mathbf{97 \pm 2}$	3.10	0.97
		QGSM	2590 ± 110	$\mathbf{84 \pm 1}$	0.91	0.99
	Central	Exper.	2734 ± 274	$\mathbf{95 \pm 2}$	1.45	0.98
		QGSM	4615 ± 348	$\mathbf{85 \pm 1}$	1.30	0.99
Boltzmann	Peripheral	Exper.	707 ± 62	$\mathbf{80 \pm 1}$	3.89	0.95
		QGSM	782 ± 42	$\mathbf{75 \pm 1}$	1.90	0.99
	Semicentral	Exper.	1180 ± 91	$\mathbf{87 \pm 1}$	4.40	0.96
		QGSM	2168 ± 87	$\mathbf{75 \pm 1}$	1.98	0.99
	Central	Exper.	2306 ± 220	$\mathbf{85 \pm 2}$	2.06	0.97
		QGSM	3862 ± 273	$\mathbf{76 \pm 1}$	1.69	0.99

were fitted by the one-temperature Hagedorn and Boltzmann functions also in range $p_t = 0.1$–0.7 GeV/c. While comparing fit results for $p_t = 0.1$–0.7 GeV/c and $p_t = 0.1$–1.2 GeV/c ranges in ^{12}C+^{12}C collisions in Ref. 28, it was observed that high p_t ($p_t > 0.7$ GeV/c) and high temperature part of the pion p_t distribution influenced significantly the extracted values of T, masking and suppressing the centrality dependence of T. The parameters extracted from fitting the p_t distributions of π^- in range $p_t = 0.1$–0.7 GeV/c by one-temperature functions for three ^{4}He+^{12}C collision centrality groups are presented in Table 8.

As seen from comparison of Tables 7 and 8, the extracted values of T in experiment proved to be noticeably lower in case of the fitting range $p_t = 0.1$–0.7 GeV/c

Table 8. The parameters extracted from fitting the p_t distributions of the negative pions in peripheral, semicentral and central ^{4}He+^{12}C collisions at $4.2A$ GeV/c by the one-temperature Hagedorn and Boltzmann functions in range $p_t = 0.1$–0.7 GeV/c.

Fitting function	Collision type	Type	A (GeV)$^{-1}$	T (MeV)	$\chi^2/n.d.f.$	R^2
Hagedorn	Peripheral	Exper.	1005 ± 101	$\mathbf{87 \pm 2}$	2.29	0.98
		QGSM	934 ± 57	$\mathbf{84 \pm 1}$	2.30	0.99
	Semicentral	Exper.	1727 ± 159	$\mathbf{93 \pm 2}$	1.89	0.99
		QGSM	2610 ± 120	$\mathbf{84 \pm 1}$	1.27	0.99
	Central	Exper.	3002 ± 343	$\mathbf{93 \pm 2}$	1.59	0.98
		QGSM	4801 ± 384	$\mathbf{84 \pm 1}$	1.62	0.99
Boltzmann	Peripheral	Exper.	847 ± 79	$\mathbf{77 \pm 1}$	3.17	0.97
		QGSM	793 ± 44	$\mathbf{74 \pm 1}$	2.65	0.99
	Semicentral	Exper.	1467 ± 126	$\mathbf{82 \pm 1}$	3.19	0.98
		QGSM	2222 ± 94	$\mathbf{74 \pm 1}$	2.88	0.99
	Central	Exper.	2594 ± 274	$\mathbf{82 \pm 2}$	2.31	0.97
		QGSM	4041 ± 298	$\mathbf{75 \pm 1}$	1.88	0.99

as compared to the fitting interval $p_t = 0.1$–1.2 GeV/c. This was most likely due to decrease of the influence of high temperature (hard p_t) component of p_t distribution of π^- to the extracted T values in going from fitting range $p_t = 0.1$–1.2 GeV/c to $p_t = 0.1$–0.7 GeV/c. On the other hand, as seen from comparison of Tables 7 and 8, the values of T obtained from QGSM spectra did not show any dependence on the fitting p_t range. As seen from Table 8, the absolute values of the spectral temperatures of the negative pions proved to be consistently and noticeably larger in case of semicentral and central collisions as compared to peripheral interactions. The temperatures extracted from QGSM spectra, as observed from Table 8, again did
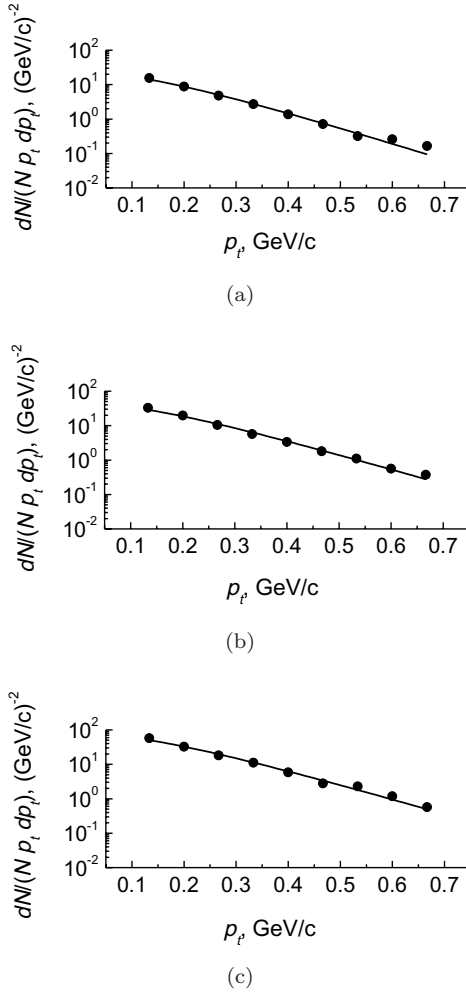

(a)

(b)

(c)

Fig. 4. The experimental transverse momentum distributions of the negative pions (•) produced in (a) peripheral, (b) semicentral and (c) central ^{4}He+^{12}C collisions at 4.2 GeV/c per nucleon and the corresponding fits in range $p_t = 0.1$–0.7 GeV/c by the one-temperature Hagedorn function (solid lines). All the spectra are normalized per one inelastic collision event.

not show any dependence on collision centrality, as was also the case for the fitting range $p_t = 0.1$–1.2 GeV/c, as seen in Table 7. Independence of QGSM temperatures on collision centrality and fitting p_t range could probably be explained by that, in QGSM the nuclear collisions were treated as superposition of independent collisions of projectile and target nucleons, stable hadrons and short-lived resonances, and the collective (nuclear) effects were not taken into account.

The experimental p_t distributions of π^- for three ^{4}He+^{12}C collision centralities and the corresponding fits in range $p_t = 0.1 - 0.7$ GeV/c by one-temperature Hagedorn function are presented in Fig. 4. As seen from Fig. 4, the one-temperature
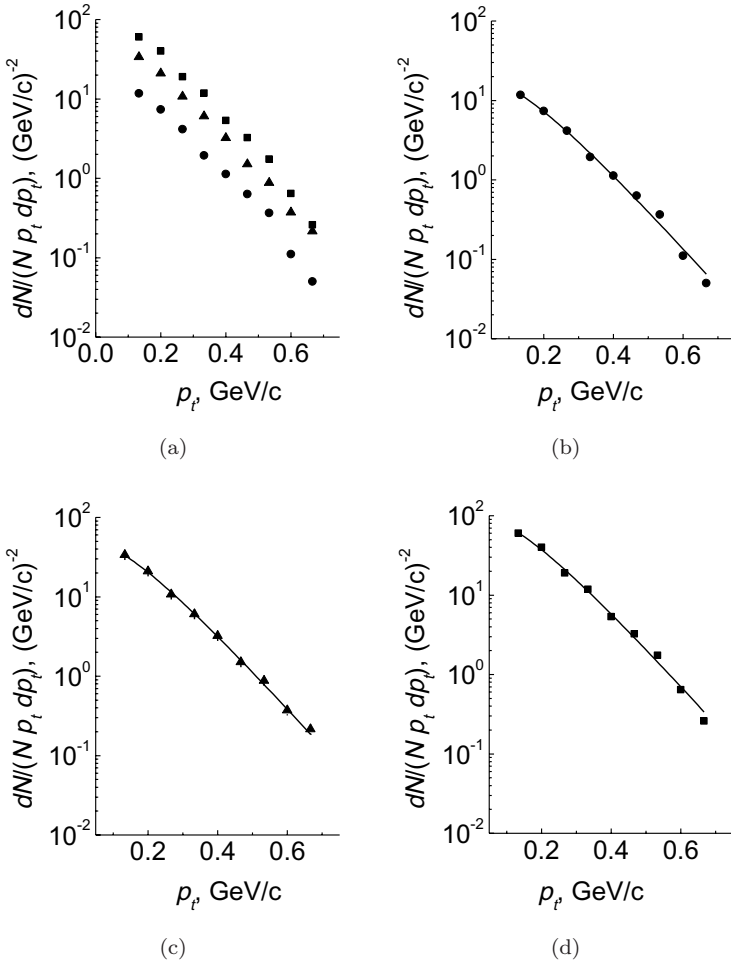
Fig. 5. The transverse momentum distributions of the negative pions calculated using QGSM for peripheral ($\bullet$) ((a) and (b)), semicentral ($\blacktriangle$) ((a) and (c)) and central ($\blacksquare$) ((a) and (d)) ^{4}He+^{12}C collisions at 4.2 GeV/c per nucleon and the corresponding fits in range $p_t = 0.1 - 0.7$ GeV/c by the one-temperature Hagedorn function (solid lines). All the spectra are normalized per one inelastic collision event.

Hagedorn function fits satisfactorily the experimental p_t distributions of the negative pions in range $p_t = 0.1$–$0.7\,\mathrm{GeV}/c$. The p_t distributions of π^- mesons, calculated using QGSM, in peripheral, semicentral and central $^4\mathrm{He}+^{12}\mathrm{C}$ collisions and the corresponding fits in range $p_t = 0.1$–$0.7\,\mathrm{GeV}/c$ by the one-temperature Hagedorn function are displayed in Fig. 5. As observed from Fig. 5, the one-temperature Hagedorn function fits quite satisfactorily the p_t distributions of the negative pions, calculated using QGSM, in three $^4\mathrm{He}+^{12}\mathrm{C}$ collision centrality groups in range $p_t = 0.1$–$0.7\,\mathrm{GeV}/c$.

According to QGSM calculations for nucleus–nucleus collisions at $4.2A\,\mathrm{GeV}/c$,[52,53] the major fraction of pions in soft p_t range originates at a later collision stage from decays of Δ resonances and vector mesons, such as ρ and ω, when the collision system cools down significantly. In soft p_t range ($p_t < 0.5\,\mathrm{GeV}/c$), according to QGSM, fraction of pions, coming from Δ and vector meson decays, increases with increasing collision system size in nucleus–nucleus collisions at $4.2A\,\mathrm{GeV}/c$.[52,53] On the other hand, the hard p_t range ($p_t > 0.5\,\mathrm{GeV}/c$), in this model, is dominated by pions produced directly in hadron–hadron collisions like $NN \to NN\pi$.[52,53] As deduced from analysis of relativistic heavy ion collisions,[54] the contribution of soft processes scales with the number of participant nucleons and that of semi(hard) scattering processes scales with the number of binary (nucleon–nucleon) collisions. As already shown in Tables 7 and 8, the QGSM temperatures, in contrast to the experimental T, were not sensitive to and did not show any dependence on collision centrality as well as the fitting range of p_t. Since the values of experimental T were sensitive both to collision centrality and fitting range of p_t, it was of interest to study the collision centrality dependences of T of soft and hard p_t components of the negative pions in experiment by fitting their p_t distributions separately in p_t ranges 0.1–$0.5\,\mathrm{GeV}/c$ and 0.5–$1.2\,\mathrm{GeV}/c$, respectively. Table 9 presents the parameters extracted from fitting by one-temperature Hagedorn and one-temperature Boltzmann functions of the experimental p_t distributions of π^- in peripheral, semicentral

Table 9. Parameters extracted from fitting by one-temperature Hagedorn and one-temperature Boltzmann functions of the experimental transverse momentum distributions of the negative pions in peripheral, semicentral and central $^4\mathrm{He}+^{12}\mathrm{C}$ collisions at $4.2A\,\mathrm{GeV}/c$ separately in ranges $p_t = 0.1$–$0.5\,\mathrm{GeV}/c$ and $p_t = 0.5$–$1.2\,\mathrm{GeV}/c$.

| | | Fitting rang | | | | | | | |
| | | $p_t = 0.1$–$0.5\,\mathrm{GeV}/c$ | | | | $p_t = 0.5$–$1.2\,\mathrm{GeV}/c$ | | | |
Fitting function	Collision type	A $(\mathrm{GeV})^{-1}$	T (MeV)	$\chi^2/$ $n.d.f.$	R^2	A $(\mathrm{GeV})^{-1}$	T (MeV)	$\chi^2/$ $n.d.f.$	R^2
Hag.	Periph.	1173 ± 148	$\mathbf{83 \pm 2}$	0.36	0.99	140 ± 47	$\mathbf{120 \pm 6}$	0.97	0.96
	Semicen.	2207 ± 267	$\mathbf{87 \pm 2}$	0.85	0.99	657 ± 19	$\mathbf{110 \pm 5}$	2.22	0.94
	Centr.	3908 ± 563	$\mathbf{87 \pm 3}$	0.44	0.99	2506 ± 122	$\mathbf{98 \pm 7}$	0.93	0.95
Bolt.	Periph.	1019 ± 116	$\mathbf{74 \pm 2}$	0.78	0.99	93 ± 2	$\mathbf{111 \pm 5}$	0.91	0.96
	Semicen.	1951 ± 213	$\mathbf{76 \pm 2}$	1.55	0.99	423 ± 11	$\mathbf{102 \pm 4}$	2.22	0.94
	Centr.	3449 ± 448	$\mathbf{76 \pm 2}$	0.67	0.99	1575 ± 729	$\mathbf{92 \pm 6}$	0.97	0.95

and central ^{4}He+^{12}C collisions at 4.2A GeV/c separately in ranges $p_t = 0.1$–0.5 GeV/c and $p_t = 0.5$–1.2 GeV/c. As can be seen from comparison of Tables 9 and 6, the separate fitting of the soft (0.1–0.5 GeV/c) and hard (0.5–1.2 GeV/c) p_t components of the negative pions resulted in lower fitting uncertainties of the extracted T as compared to combined two-temperature model fits in range $p_t = 0.1$–1.2 GeV/c. This was likely due to interplay between the temperatures of soft and hard components of pion p_t distributions in case of combined two-temperature model fits.

Soft and hard components of the experimental p_t distributions of the negative pions in peripheral, semicentral and central ^{4}He+^{12}C collisions at 4.2A GeV/c along with the corresponding fits by one-temperature Hagedorn function in p_t ranges 0.1–0.5 GeV/c and 0.5–1.2 GeV/c, respectively, are presented in Fig. 6. As seen from Fig. 6 and Table 9, both one-temperature Hagedorn and one-temperature Boltzmann functions describe satisfactorily the soft as well as hard components of p_t distributions of π^- in three centrality groups of ^{4}He+^{12}C collisions. Figure 7 demonstrates collision centrality dependences of the temperatures of soft and hard components of the experimental p_t distributions of π^- in ^{4}He+^{12}C collisions at 4.2A GeV/c, extracted from fitting by one-temperature Hagedorn function in p_t ranges 0.1–0.5 GeV/c and 0.5–1.2 GeV/c, respectively.

In semicentral and central ^{4}He+^{12}C collisions, Δ and other resonances are produced at higher energy–momentum transfers, which results in larger mean kinetic energies of pions coming from their decays as compared to those in peripheral collisions. This can explain the larger T of soft p_t component of pions in semicentral and
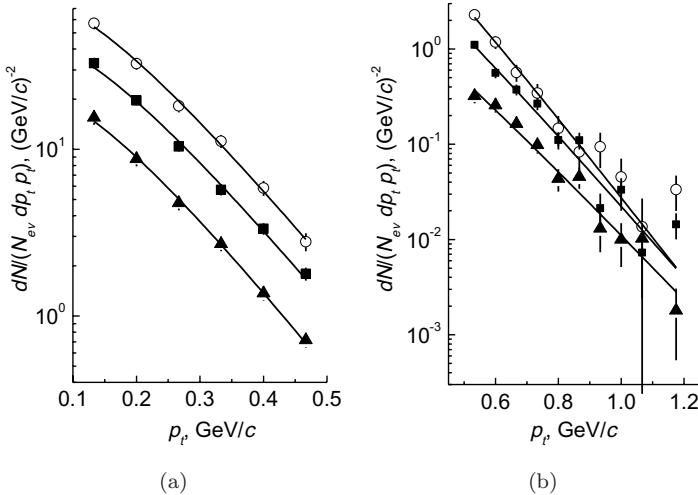

Fig. 6. (a) Soft and (b) hard components of the experimental transverse momentum distributions of the negative pions in peripheral (▲), semicentral (■), and central (○) ^{4}He+^{12}C collisions at 4.2A GeV/c along with the corresponding fits (solid lines) by the one-temperature Hagedorn function in p_t ranges 0.1–0.5 GeV/c and 0.5–1.2 GeV/c, respectively.
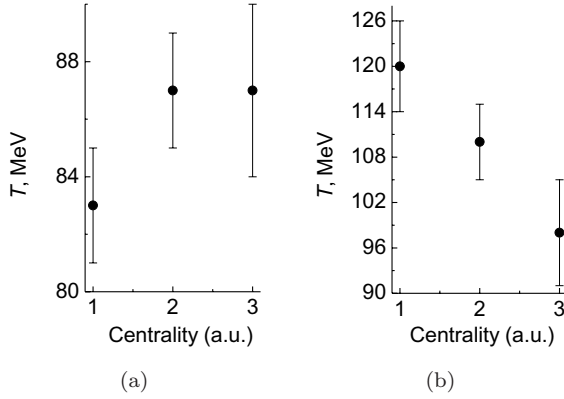
Fig. 7. Collision centrality dependence of the temperature (•) of (a) soft and (b) hard components of the experimental transverse momentum distributions of the negative pions in ^{4}He+^{12}C collisions at $4.2A$ GeV/c, extracted from fitting by the one-temperature Hagedorn function in p_t range 0.1–0.5 GeV/c and 0.5–1.2 GeV/c, respectively. The numbers 1, 2 and 3 on x-axis correspond to the group of peripheral, semicentral and central collision events, respectively.

central ^{4}He+^{12}C collisions in Fig. 7(a), as compared to the peripheral interactions. The centrality dependences of T of soft and hard p_t components of π^- in ^{4}He+^{12}C collisions, observed in Fig. 7, can be explained in terms of geometry (size) and degree of overlap of colliding nuclei. As $A_p < A_t$ in ^{4}He+^{12}C collisions, we expect a complete overlap of these colliding nuclei already in semicentral collisions. Therefore, after the initial growth of T of soft p_t component in ^{4}He+^{12}C collisions in going from peripheral to semicentral collisions, observed in Fig. 7(a), practically no more appreciable energy can be transferred from projectile to target nucleons in the range from semicentral to central collisions. Hence, the temperature of soft p_t component remains constant for semicentral and central ^{4}He+^{12}C collisions. It is necessary to add that the initial growth, followed by reaching the constant value, of the experimental T for π^- in going from peripheral to semicentral and then central ^{4}He+^{12}C collisions, respectively, was observed also in case of fitting the p_t distributions of π^- by one-temperature Hagedorn and Boltzmann functions in p_t range 0.1–0.7 GeV/c, as seen in Table 8.

As observed from Fig. 7(b), the T of hard p_t component of π^- mesons decreases consistently with an increase in ^{4}He+^{12}C collision centrality. This result is supported by centrality dependence of T_2, presented in Table 6. Despite the interplay between the temperatures T_1 and T_2 in case of combined two-temperature model fits, the value of T_2 in Table 6 also decreased consistently with increasing centrality. The decrease of T of hard p_t component with increasing centrality of ^{4}He+^{12}C collisions, observed in Fig. 7(b), can be explained in terms of semi(hard) nucleon–nucleon collisions. In case of peripheral ^{4}He+^{12}C collisions, quite energetic pions produced in semi(hard) nucleon–nucleon collisions (from small overlap zone at periphery of colliding nuclei) would most probably escape the collision zone without further rescattering. With an increase in collision centrality, the path to be traversed

through target $^{12}\mathrm{C}$ nucleus, along the direction of the impinging projectile nucleon, increases from zero to $2R(^{12}C)$ (where $R(^{12}C)$ is the radius of $^{12}\mathrm{C}$ nucleus) in going from most peripheral to most central $^4\mathrm{He}+^{12}\mathrm{C}$ collisions. Hence, the rescattering probability of a pion, produced in semi(hard) nucleon–nucleon collision, on surrounding target nucleons increases with increasing centrality of $^4\mathrm{He}+^{12}\mathrm{C}$ collisions. This could explain qualitatively the decrease of T of hard p_t component of π^- mesons with increasing centrality of $^4\mathrm{He}+^{12}\mathrm{C}$ collisions, observed in Fig. 7(b). As mentioned already, the contribution of hard processes scales with the number of binary (nucleon–nucleon) collisions, and pions in hard p_t region are produced likely in semi(hard) nucleon–nucleon collisions. Hence, such decrease of T with an increase in $^4\mathrm{He}+^{12}\mathrm{C}$ collision centrality can also be explained by an increase in the numbers of binary (nucleon–nucleon) collisions and produced pions with increasing of $^4\mathrm{He}+^{12}\mathrm{C}$ collision centrality. The pions in hard p_t range in peripheral interactions are mostly likely produced in first single semi(hard) collisions of projectile nucleons (from small overlap zone at periphery of colliding nuclei) with target nucleons at relatively large momentum–energy transfers. On the other hand, in semicentral and central collisions (since $A_p < A_t$) the collision energy of projectile nucleons is distributed among the larger number of interacting target nucleons and produced pions as compared to peripheral interactions, which can bring about the decrease of the average kinetic energy (and, hence, temperature) of produced pions in hard p_t region with an increase in $^4\mathrm{He}+^{12}\mathrm{C}$ collision centrality.

Figure 8 displays collision centrality dependences of T of soft and hard components of the experimental p_t distributions of π^- in $^4\mathrm{He}+^{12}\mathrm{C}$ collisions at $4.2A\,\mathrm{GeV}/c$, extracted from fitting by one-temperature Boltzmann function in p_t ranges 0.1–$0.5\,\mathrm{GeV}/c$ and 0.5–$1.2\,\mathrm{GeV}/c$, respectively. As seen from Fig. 8, the temperatures extracted from one-temperature Boltzmann function reproduce completely the behavior of centrality dependences of T of both soft and hard p_t components of π^- in $^4\mathrm{He}+^{12}\mathrm{C}$ collisions, observed in Fig. 7.
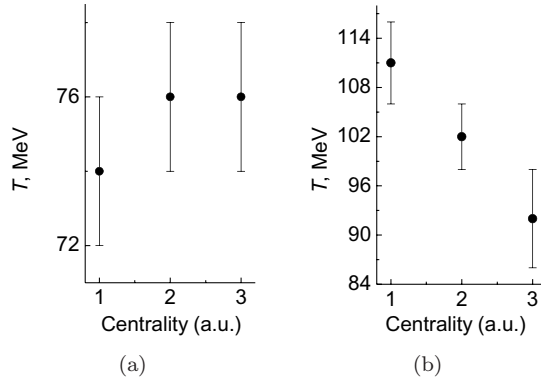

Fig. 8. The same as in Fig. 7, but extracted from fitting by the one-temperature Boltzmann function.

Finally, it is of importance to discuss some quantitative results on temperatures of pions, obtained in other JINR (Joint Institute for Nuclear Research), GSI (Gesellschaft for Schwerionenforschung) and SPS (Super Proton Synchrotron) experiments in order to link the findings of the present work with those obtained at lower, intermediate and higher energies. In Ref. 55, the temperatures of the negative pions in central Mg+Mg collisions at $4.3A\,\mathrm{GeV}/c$ (GIBS set-up of JINR) were estimated from inclusive kinetic energy and transverse momentum spectra of π^- mesons using two different selection criteria: In the rapidity interval 0.5–2.1 (corresponding to π^- pionization region) and at cms (center-of-mass system) angles $(90 \pm 10)°$. The pion spectra were fitted by a sum of two exponentials with two temperatures, $T_1 = 55 \pm 1\,\mathrm{MeV}$ and $T_2 = 113 \pm 2\,\mathrm{MeV}$. The relative yield of T_2 was about 22%. The two-temperature behavior of spectra was explained by two mechanisms: Direct production (T_2) of π^-, and production of π^- via decay of Δ (T_1). These values of T_1 and T_2 are comparable with the corresponding temperatures of the negative pions in central $^4\mathrm{He}+^{12}\mathrm{C}$ collisions at $4.2A\,\mathrm{GeV}/c$ extracted in the present work (see Table 6). The light front analysis of the negative pions in central He(Li, C), C+Ne, C+Cu and O+Pb collisions at $4.5A\,\mathrm{GeV}/c$ was made in Ref. 56. The phase space of secondary pions was divided into two parts, into one of which the thermal equilibrium seemed to be in a good agreement with the data. The thermal equilibrium region corresponded to lower p_t range.[56] The corresponding temperatures were extracted and their dependence on system size $(A_p A_t)^{1/2}$ was studied. The extracted temperatures proved to be 81 ± 2, 79 ± 3, 72 ± 2 and $55 \pm 3\,\mathrm{MeV}$ in central He(Li, C), C+Ne, C+Cu and O+Pb collisions at $4.5A\,\mathrm{GeV}/c$, respectively.[56] The temperature decreased with an increase in system size. The temperature obtained in central He(Li, C) collisions at $4.5A\,\mathrm{GeV}/c$ is compatible with the temperature of soft p_t component of π^- mesons in central $^4\mathrm{He}+^{12}\mathrm{C}$ collisions at $4.2A\,\mathrm{GeV}/c$, extracted in the present analysis (see Table 9).

The temperatures of pions were extracted also in GSI experiments (FOPI, FRS, KAON and TAPS Collaborations).[57–62] It was obtained that the spectra of π^- mesons in central Ni+Ni collisions at incident (kinetic) energies $E_{\mathrm{kin}} = 1.06A\,\mathrm{GeV}$, $1.45A\,\mathrm{GeV}$ and $1.93A\,\mathrm{GeV}$ (FOPI Collaboration[57]) required the sum of two exponentials with independent yields and inverse slope parameters T_l and T_h describing mainly the low and high momentum part of the spectrum, respectively. $T_l = 55 \pm 3\,\mathrm{MeV}$ and $T_h = 93 \pm 5\,\mathrm{MeV}$, $T_l = 56 \pm 3\,\mathrm{MeV}$ and $T_h = 100 \pm 5\,\mathrm{MeV}$ and $T_l = 61 \pm 3\,\mathrm{MeV}$ and $T_h = 115 \pm 6\,\mathrm{MeV}$ were extracted at $E_{\mathrm{kin}} = 1.06A\,\mathrm{GeV}$, $1.45A\,\mathrm{GeV}$ and $1.93A\,\mathrm{GeV}$, respectively. In Ne+NaF collisions (FRS Collaboration), the T for π^- mesons ranged from $78 \pm 2\,\mathrm{MeV}$ to $96 \pm 3\,\mathrm{MeV}$ for projectile energies from $1.34A\,\mathrm{GeV}$ to $1.94A\,\mathrm{GeV}$. The KAON Collaboration extracted the value of T for π^+ mesons to be $71 \pm 3\,\mathrm{MeV}$ and $95 \pm 3\,\mathrm{MeV}$ for projectile energies $1A\,\mathrm{GeV}$ and $1.8A\,\mathrm{GeV}$, respectively. The TAPS Collaboration obtained T value for π^0 mesons to be $83 \pm 3\,\mathrm{MeV}$ in C+C collisions at $E_{\mathrm{kin}} = 2A\,\mathrm{GeV}$ and $T = 70 \pm 1\,\mathrm{MeV}$ in Ar+Ca

collisions at $E_{\mathrm{kin}} = 1.5A$ GeV. Significantly larger inverse slope parameters (apparent temperatures) T ranging from around 140 MeV to 160 MeV were extracted in SPS experiments by NA44 Collaboration[48,63] for charged pions from fitting their transverse mass spectra with simple Boltzmann distribution in central Pb+Pb and S+S collisions at $158A$ GeV/c and $200A$ GeV/c, respectively.

Summarizing, on the whole, the temperatures extracted from pion spectra in central nucleus–nucleus collisions (GSI, JINR, SPS experiments) depended on collision energy and sizes (geometry) of colliding nuclei.

3. Summary and Conclusion

The p_t distributions of the negative pions in minimum bias ^{4}He+^{12}C collisions at $4.2A$ GeV/c, as well as in selected ^{4}He+^{12}C collision centralities, were analyzed systematically by fitting the corresponding p_t distributions with the one- and two-temperature Hagedorn and Boltzmann functions in various p_t ranges. We observed that the p_t distributions of π^- required two-temperature function fits for their adequate description in the whole p_t range as well as in the fitting interval $p_t = 0.1$–1.2 GeV/c, in agreement with the earlier results obtained for different sets of colliding nuclei at relativistic energies.[19–21,23,24,27–29,55,57]. The spectral temperatures (T_1, T_2) of π^- mesons in minimum bias ^{4}He+^{12}C collisions at $4.2A$ GeV/c and their relative contributions (R_1, R_2) were extracted from fitting their total p_t distribution in the whole p_t range by the two-temperature Hagedorn and Boltzmann functions. The dominant contribution $(R_1 \sim 90\%)$ to the total π^- multiplicity in minimum bias ^{4}He+^{12}C collisions was given by $T_1 \sim (68 - 83) \pm 5$ MeV. The values of the spectral temperatures (T_1, T_2) extracted in the present work from fitting the p_t distribution by the two-temperature Hagedorn and Boltzmann functions were noticeably lower than the corresponding values obtained in Ref. 19 (on less than half of the collision statistics used in the present analysis) from fitting the noninvariant cm energy spectrum of π^- in ^{4}He+^{12}C collisions at $4.2A$ GeV/c by Maxwell–Boltzmann distribution function.

We extracted and fitted the p_t distributions of the negative pions for three different ^{4}He+^{12}C collision centralities in ranges $p_t = 0.1$–1.2 GeV/c and $p_t = 0.1$–0.7 GeV/c. On the whole, the absolute values of the extracted temperatures were lower in case of fitting in range $p_t = 0.1$–0.7 GeV/c as compared to the fitting interval $p_t = 0.1$–1.2 GeV/c. This was likely due to decrease of the influence of high temperature (hard p_t) component of p_t distribution of π^- to the extracted T value in going from fitting range $p_t = 0.1$–1.2 GeV/c to $p_t = 0.1$–0.7 GeV/c. The one-temperature Hagedorn and Boltzmann functions were sufficient for fitting satisfactorily the experimental p_t spectra of the negative pions in the range $p_t = 0.1$–0.7 GeV/c. The extracted QGSM temperatures did not depend on collision centrality and fitting p_t range. As contrasted to the QGSM temperatures, the temperatures obtained from the experimental p_t distributions were sensitive to collision

centrality and fitting range of p_t. Independence of QGSM temperatures on collision centrality and fitting p_t range was explained by that, in QGSM the nuclear collisions were treated as superposition of independent collisions of projectile and target nucleons, stable hadrons and short-lived resonances, and the collective (nuclear) effects were not accounted for.

We analyzed the collision centrality dependences of the temperatures of soft $(p_t = 0.1\text{--}0.5\,\text{GeV}/c)$ and hard $(p_t = 0.5\text{--}1.2\,\text{GeV}/c)$ components of the experimental p_t distributions of the negative pions in $^4\text{He}+^{12}\text{C}$ collisions at $4.2A\,\text{GeV}/c$. For the selected three collision centrality groups, the temperatures were extracted from fitting separately the soft and hard components of p_t distributions of π^- mesons by one-temperature Hagedorn and Boltzmann functions. The temperatures extracted using one-temperature Boltzmann function reproduced completely the observed collision centrality dependences of the temperatures of both soft and hard p_t components, obtained from fitting by one-temperature Hagedorn function. The extracted temperatures of both soft and hard components of p_t distributions of π^- depended on geometry (size) and degree of overlap of colliding nuclei in peripheral, semicentral and central $^4\text{He}+^{12}\text{C}$ collisions. The temperature of soft p_t component of the negative pions was consistently larger in semicentral and central $^4\text{He}+^{12}\text{C}$ collisions than that in peripheral interactions. This result was supported by similar centrality dependence of T obtained in case of one-temperature fits in range $p_t = 0.1\text{--}0.7\,\text{GeV}/c$. The observed centrality dependence of T of soft p_t component of the negative pions was explained as follows. In contrast to peripheral interactions, in semicentral and central $^4\text{He}+^{12}\text{C}$ collisions, Δ and other resonances are produced at higher energy–momentum transfers, resulting in larger mean kinetic energies of pions coming from their decays as compared to those in peripheral collisions. Hence, the T of soft p_t component of π^- should be larger in semicentral and central $^4\text{He}+^{12}\text{C}$ collisions as compared to T in peripheral interactions. The temperature of hard p_t component of π^- in $^4\text{He}+^{12}\text{C}$ collisions decreased consistently with an increase in collision centrality. This result was confirmed by similar decrease of T_2 with increasing centrality observed in case of combined two-temperature model fits in range $p_t = 0.1\text{--}1.2\,\text{GeV}/c$. Such decrease of T of hard p_t component of the negative pions could be explained by an increase in rescattering probability of a pion, produced in semi(hard) nucleon–nucleon collision, on surrounding target nucleons with increasing centrality of $^4\text{He}+^{12}\text{C}$ collisions. This decrease of T of hard p_t component of π^- in $^4\text{He}+^{12}\text{C}$ collisions can also be explained by an increase in the numbers of binary (nucleon–nucleon) collisions and produced pions with increasing of $^4\text{He}+^{12}\text{C}$ collision centrality. In semicentral and central collisions (since $A_p < A_t$), the collision energy of projectile nucleons has to be distributed among the larger number of interacting target nucleons and produced pions as compared to peripheral interactions, which is likely to result in decrease of the average kinetic energy (and, hence, temperature) of produced pions in hard p_t region with an increase in $^4\text{He}+^{12}\text{C}$ collision centrality.

Acknowledgments

We are thankful to the staff of the Laboratory of High Energies of JINR (Dubna, Russia) and of the Laboratory of Multiple Processes of Physical-Technical Institute of Uzbek Academy of Sciences (Tashkent, Uzbekistan), who participated in the processing of stereophotographs from 2 m propane bubble chamber of JINR and increasing significantly the corresponding statistics of nucleus–nucleus collisions at 4.2A GeV/c. We are grateful to N. Amelin (JINR) for providing us the data of simulated QGSM collision events. A. I. and M. Q. H. acknowledge the partial support from HEC (Higher Education Commission of Pakistan) Research Project No. 1925.

References

1. P. Braun-Munzinger and J. Stachel, *Annu. Rev. Nucl. Part. Sci.* **37** (1987) 97.
2. J. W. Harris *et al.*, *Phys. Lett. B* **153** (1985) 377.
3. R. Stock, *Phys. Rep.* **135** (1986) 259.
4. R. Stock *et al.*, *Phys. Rev. Lett.* **49** (1982) 1236.
5. Kh. K. Olimov, M. Q. Haseeb, I. Khan, A. K. Olimov and V. V. Glagolev, *Phys. Rev. C* **85** (2012) 014907.
6. Kh. K. Olimov, M. Q. Haseeb and I. Khan, *Phys. At. Nucl.* **75** (2012) 479.
7. Kh. K. Olimov *et al.*, *Phys. Rev. C* **75** (2007) 067901.
8. Kh. K. Olimov and M. Q. Haseeb, *Eur. Phys. J. A* **47** (2011) 79.
9. Kh. K. Olimov, M. Q. Haseeb, A. K. Olimov and I. Khan, *Cent. Eur. J. Phys.* **9** (2011) 1393.
10. D. Krpic, G. Skoro, I. Picuric, S. Backovic and S. Drndarevic, *Phys. Rev. C* **65** (2002) 034909.
11. Kh. K. Olimov, *Phys. Rev. C* **76** (2007) 055202.
12. Kh. K. Olimov, S. L. Lutpullaev, B. S. Yuldashev, Y. H. Huseynaliyev and A. K. Olimov, *Eur. Phys. J. A* **44** (2010) 43.
13. Kh. K. Olimov, *Phys. At. Nucl.* **73** (2010) 433.
14. B.-A. Li and C. M. Ko, *Phys. Rev. C* **52** (1995) 2037.
15. W. Ehehalt, W. Cassing, A. Engel, U. Mosel and Gy. Wolf, *Phys. Lett. B* **298** (1993) 31.
16. FOPI Collab. (M. Eskef *et al.*), *Eur. Phys. J. A* **3** (1998) 335.
17. E814 Collaboration (J. Barrette *et al.*), *Phys. Lett. B* **351** (1995) 93.
18. G. E. Brown, J. Stachel and G. M. Welke, *Phys. Lett. B* **253** (1991) 19.
19. S. Backovic *et al.*, *Phys. Rev. C* **46** (1992) 1501.
20. Kh. K. Olimov, M. Q. Haseeb and S. A. Hadi, *Int. J. Mod. Phys. E* **22** (2013) 1350020.
21. R. Brockmann *et al.*, *Phys. Rev. Lett.* **53** (1984) 2012.
22. L. Chkhaidze *et al.*, *Z. Phys. C* **54** (1992) 179.
23. B. Li and W. Bauer, *Phys. Rev. C* **44** (1991) 450.
24. L. Chkhaidze, T. Djobava and L. Kharkhelauri, *Bull. Georg. Natl. Acad. Sci.* **4** (2010) 41.
25. L. Chkhaidze *et al.*, *Nucl. Phys. A* **831** (2009) 22.
26. R. Hagedorn and J. Rafelski, *Phys. Lett. B* **97** (1980) 136.
27. Kh. K. Olimov and M. Q. Haseeb, *Phys. At. Nucl.* **76** (2013) 595.
28. A. Iqbal *et al.*, *Int. J. Mod. Phys. E* **23** (2014) 1450047.
29. Kh. K. Olimov *et al.*, *Int. J. Mod. Phys. E* **23** (2014) 1450084.

30. Kh. K. Olimov, A. Iqbal, V. V. Glagolev and M. Q. Haseeb, *Phys. Rev. C* **88** (2013) 064903.
31. Lj. Simic *et al.*, *Phys. Rev. C* **52** (1995) 356.
32. A. I. Bondarenko *et al.*, *Phys. At. Nucl.* **65** (2002) 90.
33. L. Chkhaidze, T. Djobava and L. Kharkhelauri, *Bull. Georg. Natl. Acad. Sci.* **6** (2012) 44.
34. Kh. K. Olimov, S. L. Lutpullaev, A. K. Olimov, V. I. Petrov and S. A. Sharipova, *Phys. At. Nucl.* **73** (2010) 1847.
35. L. Chkhaidze, P. Danielewicz, T. Djobava, L. Kharkhelauri and E. Kladnitskaya, *Nucl. Phys. A* **794** (2007) 115.
36. G. N. Agakishiyev *et al.*, *Z. Phys. C* **27** (1985) 177.
37. D. Armutlisky *et al.*, *Z. Phys. A* **328** (1987) 455.
38. A. I. Bondarenko *et al.*, The Ensemble of interactions on carbon and hydrogen nuclei obtained using the 2 m propane bubble chamber exposed to the beams of protons and H-2, He-4, C-12 relativistic nuclei at the Dubna Synchrophasotron, JINR Communications No. P1-98-292, JINR, Dubna (1998).
39. V. D. Toneev, N. S. Amelin, K. K. Gudima and S. Yu. Sivoklokov, *Nucl. Phys. A* **519** (1990) 463c.
40. N. S. Amelin, K. K. Gudima, S. Yu. Sivoklokov and V. D. Toneev, *Sov. J. Nucl. Phys.* **52** (1990) 172.
41. N. S. Amelin, K. K. Gudima and V. D. Toneev, *Sov. J. Nucl. Phys.* **51** (1990) 1093.
42. N. S. Amelin, E. F. Staubo, L. P. Csernai, V. D. Toneev and K. K. Gudima, *Phys. Rev. C* **44** (1991) 1541.
43. B. Gankhuyag and V. V. Uzhinskii, *Czech. J. Phys.* **47** (1997) 913.
44. A. S. Galoyan, G. L. Melkumov and V. V. Uzhinskii, *Phys. A. Nucl.* **65** (2002) 1722.
45. A. S. Galoyan *et al.*, *Phys. At. Nucl.* **66** (2003) 836.
46. Ts. Baatar *et al.*, *Phys. At. Nucl.* **63** (2000) 839.
47. R. Hagedorn and J. Ranft, *Suppl. Nuovo Cimento* **6** (1968) 169.
48. NA44 Collab. (I. Bearden *et al.*), *Phys. Rev. Lett.* **78** (1997) 2080.
49. L. Chkhaidze *et al.*, *Phys. Rev. C* **84** (2011) 064915.
50. L. V. Chkhaidze *et al.*, *Phys. At. Nucl.* **67** (2004) 693.
51. S. Backovic *et al.*, *Sov. J. Nucl. Phys.* **50** (1989) 1001.
52. R. N. Bekmirzaev *et al.*, *Phys. At. Nucl.* **58** (1995) 58.
53. R. N. Bekmirzaev *et al.*, *Phys. At. Nucl.* **58** (1995) 1721.
54. STAR Collab. (B. I. Abelev *et al.*), *Phys. Rev. C* **79** (2009) 034909.
55. L. Chkhaidze *et al.*, *J. Phys. G* **22** (1996) 641.
56. M. Anikina *et al.*, *Eur. Phys. J. A* **7** (2000) 139.
57. B. Hong *et al.*, *Phys. Rev. C* **57** (1998) 244.
58. A. Gilg *et al.*, GSI Scientific Report 96-1, GS1 Helmholtz Center for Heavy Ion Research, Darmstadt (1996), p. 52.
59. M. Pfeiffer *et al.*, GSI Scientific Report 93-1, GS1 Helmholtz Center for Heavy Ion Research, Darmstadt (1993), p. 58.
60. O. Schwalb *et al.*, GSI Scientific Report 93-1, GS1 Helmholtz Center for Heavy Ion Research, Darmstadt (1993), p. 62.
61. M. Appenheimer *et al.*, GSI Scientific Report 97-1, GS1 Helmholtz Center for Heavy Ion Research, Darmstadt (1997), p. 58.
62. C. Muntz *et al.*, GSI Scientific Report 95-1, GS1 Helmholtz Center for Heavy Ion Research, Darmstadt (1995), p. 77.
63. N. Herrmann, J. P. Wessels and T. Wienold, *Annu. Rev. Nucl. Part. Sci.* **49** (1999) 581.